TRIBOLOGY TRANSACTIONS
2020, VOL. 63, NO. 6, 1051–1066
https://doi.org/10.1080/10402004.2020.1788195

stle
Society of Tribologists and Lubrication Engineers

Minimum Energy Hypothesis in Quasi-Static Equilibrium Solutions for Angular Contact Ball Bearings

Pradeep K. Gupta

PKG Inc., Clifton Park, NY, USA

ABSTRACT

The commonly used quasi-static model for angular contact bearings is enhanced by coupling contact mechanics and bearing kinematic analyses with traction or friction behavior in ball–race contacts. The points of pure rolling in the contacts, which constitute the primary inputs in the kinematic equations, are determined by minimizing the frictional dissipation based on a prescribed elastohydrodynamic traction model. Such an intricate coupling between contact mechanics, bearing kinematics, and lubricant behavior provides significant enhancement of simple quasi-static model for greatly improved prediction of traction behavior and heat generation in ball bearing contacts. The predictions are in close agreement with those obtained by much more sophisticated dynamic analysis based on integration of classical differential equations of motion of bearing elements. The enhanced quasi-static model can therefore be effectively used as a design tool for optimizing thermal dissipation in ball–race contacts in ball bearings. To facilitate immediate evaluation and implementation of the model to practical problems, a standalone software, containing the enhanced quasi-static model, is made freely available at www.PradeepKGuptaInc.com/AdoreQS.html.

ARTICLE HISTORY
Received 26 November 2019
Accepted 22 June 2020

KEYWORDS
Quasi-static rolling bearings models; race control hypothesis; bearing heat generation; rolling bearing wear prediction; ADORE; AdoreQS

Introduction

The high load-carrying capacity, stiffness, and relatively small size make rolling bearings the most commonly used type of bearings in rotating machinery operating over a wide range of loads and speeds. The main shaft bearings in gas turbine engines constitute the most critical components in the entire propulsion system. Realistic performance simulation of these bearings requires a close integration of several disciplines. As the operating loads and speeds are imposed on the bearings, contact mechanics define the geometry of contacts and the applicable stresses, lubricant behavior in the contacts determines the frictional interactions in the contact, and the resulting accelerations are input to the dynamic equations of motion of the bearing elements. Though each one of these interactions is quite simple and well defined, it is the intricate coupling between the interactions that makes realistic performance modeling of the bearing a difficult task. For example, in a ball bearing, as the inner race begins to turn, slip is introduced in the ball–race contacts and the applicable rheological behavior of the lubricant in the contacts results in traction, which in turn imposes acceleration on the ball and the ball begins to turn and move around the bearing. As the ball travels around the bearing, any changes in contact loads alter both the contact stress and geometry and impose additional cyclic acceleration. In the meantime, the frictional dissipation in the contact produces heat, which affects the lubricant temperature. The varying lubricant temperature affects both lubricant traction and the overall temperature field in the bearing. The varying temperatures in the bearing, in addition to altering the rheological behavior of the lubricant, may also affect applicable properties of the bearing materials and bearing geometry, both of which are inputs to the contact mechanics model. Thus, an intricate coupling between tribology, contact mechanics, and dynamics determines the behavior of the ball bearing in a prescribed operating environment. When a definite quantity of lubricant circulates through the bearing, as commonly seen in turbine engine bearings, the applicable fluid mechanics models lead to lubricant drag forces and churning moments, which in addition to affecting the applied forces and moments on the moving bearing elements, greatly affect heat generation in the bearing. Thus, in addition to tribology, contact mechanics, and dynamics, the principals of fluid mechanics and heat transfer also play an important role in modeling the performance of a rolling bearing.

The first bearing performance model may be attributed to Jones (*1*, *2*), where a simple contact mechanics formulation is used to compute the contact stresses, bearing kinematics define the overall angular velocities of the rolling element, and the governing equations are restricted to static equilibrium of all forces and moments. Because the applicable centrifugal forces, corresponding to the computed kinematic orbital angular velocities of the rolling elements, are included in the applied forces in the static equilibrium

CONTACT Pradeep K. Gupta guptap@pradeepkguptainc.com
Review led by Y.S. Kang.

Nomenclature

a	Major contact half-width (m)	r	Radial coordinate (m)
F	Force (N)	T	Temperature (K)
G	Effective shear modulus (Pa)	x	Axial coordinate (m).
h	Lubricant film thickness (m)	α	Contact angle (°)
I	Moment of inertia (kgm/m^2)	β	Orientation of ball angular velocity vector (°)
K	Thermal conductivity (W/m/K)	$\dot{\gamma}$	Strain rate (1/s)
M	Moment (N.m)	θ	Orbital coordinate (°)
m	Mass (kgm)	μ	Viscosity (Pa.s)
N	Number of balls in the bearing	τ	Shear stress (Pa)
n	Shear-thinning exponent	ψ	Azimuth angle (°)
p	Pressure (Pa)	ω	Ball angular velocity (1/s)
Q	Load (N)		
q	Frictional dissipation or heat generation in ball–race contacts (W)		

equations, the model is commonly referred to as quasi-static. The purpose of this pioneering work is to provide a realistic estimate of load distribution over the rolling elements, overall bearing stiffness, and anticipated subsurface fatigue life of the bearing. The computer codes developed by Jones *(1, 2)* are still widely used throughout the bearing industry for simple bearing designs. Following the work of Jones *(1, 2)*, contact mechanics, kinematics, and force and moment equilibrium solutions applicable to all types of rolling bearings have been documented in the landmark work of Harris *(3)*. With the realization that in most turbine engine bearing applications, where the lubricant flows through the bearing, a significant fraction of the heat generation results from shearing of the lubricant as the bearing elements move around the bearing, Rumbarger et al. *(4)* developed simple models to simulate these fluid effects. The models are based on the classical laminar and turbulent fluid flow over cylindrical and spherical bodies as documented by Schlichtig *(5)*. The work of Crecelius and Pirvics *(6)* and the related bearing performance code SHABERTH extend the quasi-static equilibrium solutions to implement the lubricant churning moments and drag forces, based on kinematic angular velocities of bearing elements, and establish a groundwork for thermal interactions of the bearing with rest of the system. SHABERTH provides another milestone for the quasi-static bearing performance models and is also currently widely used for overall bearing system design. In more recent years, the bearing code COBRA, developed by Poplawski *(7)*, has become quite popular for quasi-static bearing solution. In addition to modeling multiple bearings on a shaft, similar to SHABERH, COBRA can be interfaced with a finite element model for overall rotor–bearing system design. It is therefore currently a popular design code.

Over the past several decades there has been significant development in the area of tribological behavior of concentrated rolling element–to-race contacts. Lubricant rheology in high-pressure contacts, the effective lubricant film thickness, and the resulting traction forces under prescribed slip rates are now fairly well understood. Realistic relations between slip and traction may now be reliably calculated from independently measured rheological behavior of the lubricant. The works of Hamrock and Dowson *(8)* and Bair *(9)* provide a comprehensive review of the current state of the art. Because all angular velocities in the current quasi-static equilibrium models are computed by kinematic considerations, realistic slip in the ball-to-race contacts cannot be truly defined. Hence, the models are somewhat weak in interfacing with the tribological behavior in the concentrated contacts determined by the contact mechanics solutions for ball-to-race interactions. Truly dynamic models based on the integration of classical differential equations of motion of bearing elements, on the other hand, are free of any kinematic considerations. Under any prescribed forces and moments, the bearing elements are permitted to accelerate arbitrarily and the differential equations of motion are integrated in time to determine the applicable steady-state solution. Because the integration of differential equations is often required over relatively large time domains, these models are generally quite computationally intensive. Therefore, in early times the practical use of these models was greatly restricted by the required computing effort. However, with the recent advances in computing hardware and several orders of magnitude increase in computing speeds, the required computing effort no longer poses any practical limitation. Hence, a realistic interface of tribological behavior with contact mechanics is now possible, which has resulted in significant advancement of rolling bearing performance models.

The first dynamic model, based on differential equations of motion, for a ball bearing may be attributed to to Walters *(10)*. This work was primarily prompted by observed instabilities in the motion of a bearing cage. Therefore, while the cage is modeled with complete six-degrees-of-freedom motion, the ball mass center is constrained to move along the path determined by the force equilibrium solution. However, the equations of motion for ball orbital and angular velocities are implemented with complete generality. Hence, this work does provide a realistic interface with tribological behavior at the rolling element-to-race contacts. In fact, it is found that the ball–race tribological behavior is a key input in defining stability of cage motion. Following this work, Gupta *(11)* presented a fully generalized dynamic model for all types of rolling bearings with a fairly comprehensive interface with a lubricant traction model. This work

has been subsequently advanced to the current bearing dynamics code ADORE *(12)* (*Advanced Dynamics of Rolling Elements*). Although ADORE was first published in 1984, it has been continually advanced over the last several decades and is perhaps the most widely used bearing dynamics model. In addition to the works reviewed above, there have been a number of other notable advancements in both the quasi-static equilibrium and real-time dynamics models for rolling bearings. Gupta *(13)* has presented an extensive review of the advancements in the subject.

When solving the equilibrium problem, a solution to the force equilibrium equations determines the contact load, angles, and geometry. This constitutes only half of the problem, because it is also essential to compute angular velocities of the rolling elements under prescribed race velocities. Jones *(1)* developed a fairly rigorous friction moment equilibrium formulation in terms of the contact load and ball angular velocities in an angular contact ball bearing. Even under a constant coefficient, because the Hertzian contact solution involves elliptical integrals, integration of the friction moment over the ball–race contact became numerically quite complex. With limited computing capabilities at the time, the analytical complexity of this formulation made the solution procedures extremely difficult. However, by noting that the gyroscopic moment on the ball is quite small in comparison to the moment exerted by the friction forces, Jones *(1)* was able to greatly simplify the solution procedures by neglecting the gyroscopic moment. These solutions revealed that spin, or relative angular velocity about the load axis normal to the plane of contact, exists only on one of the races, which provides lesser of the spin moment. Thus, Jones *(1)* introduced the concept of "race control" for computation of ball angular velocities in quasi-static equilibrium models. The race that only has rolling and no relative spin is defined as the "controlling race." The race control hypothesis remains as the current state-of-the-art in modeling ball angular velocities in quasi-static equilibrium models for angular contact ball bearings.

Though early experimental work carried out by Shevchenko and Bolan *(14)* provides some support to the race control hypothesis, Hirano *(15)* demonstrated that under high-speed conditions only the ball orbital angular velocity (equivalent of cage angular velocity) as predicted by the outer race control hypothesis is in agreement with the experimental data and it is essential to consider the gyroscopic moment to justify the experimentally observed skewed roll axis of the ball. However, the experiments were carried out under well-lubricated conditions where the equivalent friction coefficient may not only be relatively low but dependent on slip velocity under prescribed contact stress and operating temperature. Anderson *(16)* used the term "ball control" because the ball motion is essentially controlled by controlling the race on which there is pure rolling. Again, in the absence of any gyroscopic effects, it is stated that ball control moves from the inner race to the outer race as the centrifugal force increases with increasing operating speed and the outer race contact becomes more heavily loaded.

Kingsbury *(17, 18)* carried out experimental work with an angular contact ball bearing with a cage and concluded that the ball motion is controlled by the race in terms of ball–race slip but the friction moment generated at the ball–cage contacts controls relative ball spin. Gupta *(19)*, while discussing the experimental results obtained by Kingsbury *(18)*, pointed out that the bored balls used in the experiments, to facilitate angular velocity measurements, have a preferred axis of inertia, which may affect ball motion, and by carrying out a dynamic simulation it is demonstrated that the preferred axis of inertia contributes to notable ball precession. However, Kingsbury *(18)* confirmed that the bore has no significant impact on ball motion unless the ball goes through excessive precession due to lubrication effects. Ai and Moyer *(20)* discussed the concept of a minimum differential slip hypothesis, which could approximate minimum frictional dissipation when the relative spin angular velocities at the outer and inner races are equal and opposite in the absence of any gross sliding. The dissipation is minimum when the spin moments on the races are equal. Such a condition may be difficult to achieve in an angular contact ball bearing when the contact loads and angles are different on the outer and inner races due to centrifugal effects. The condition may be possible in a radially loaded ball bearing when the ball is pure rolling on both races and there are no spin moments in either contact.

From the above developments, it is clear that even under a constant friction coefficient, the formulation and solution of any type of moment equilibrium equation to determine the ball angular velocities in an angular contact ball bearing are difficult and numerically complex. A dynamic simulation, where the equations of motion are integrated in the time domain, with arbitrary initial conditions, is the best approach to obtain a steady-state solution. With such a dynamic approach, the most realistic elastohydrodynamic behavior at the ball–race contacts, along with all gyroscopic effects in any arbitrary operating environment, may be modeled. However, a number of common design parameters, such as bearing fatigue life, overall load distribution, and bearing stiffness, are insensitive to subtle angular velocity variations and related dynamic effects, and these parameters can be very easily and efficiently determined by quasi-static equilibrium solutions. However, the missing element in the quasi-static formulation is a realistic estimate of frictional dissipation in the ball–race contacts, which of course is related to subtle velocity variations and tribological behavior in the contacts. With due recognition of such a limitation, Gupta *(21)* proposed a minimum energy hypothesis as a replacement for the currently used empirical race control hypothesis. The concept is based on the commonly used minimum energy principal. However, the implementation of the hypothesis adds another level of numerically intensive iterations in the equilibrium formulation. In view of limitations on computing speed at the time, this posed notable restrictions on practical use of the model. With the recent advances in computing hardware, such sophistication in bearing performance models is now within practical reach. Thus, the objective of the present investigation is to further develop the minimum energy hypothesis, implement the hypothesis in a quasi-static equilibrium model, and evaluate the results against the steady-state solution obtained with a generalized dynamic simulation. It is expected that such an enhancement will provide more realistic

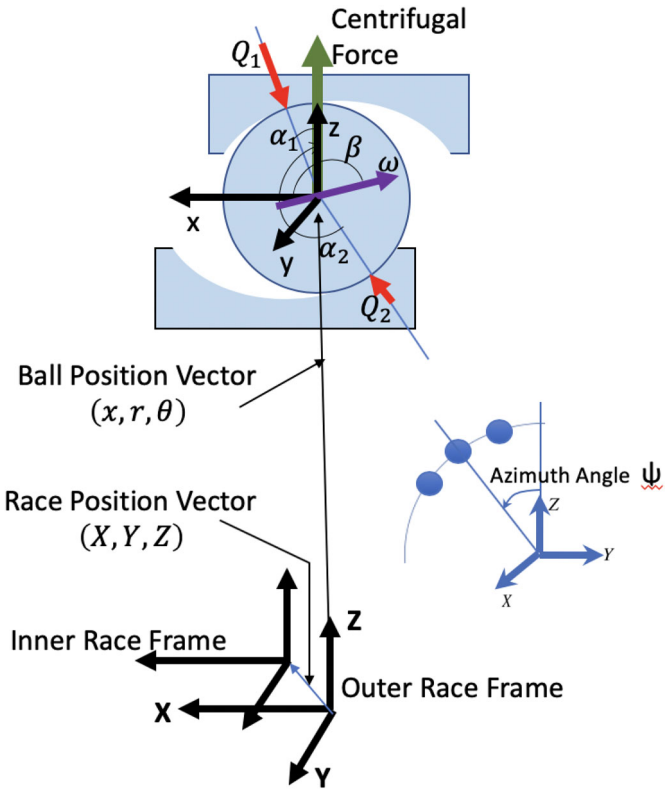

Figure 1. Schematic description of ball–race contact.

quasi-static solutions for optimization of bearing designs where heat generation in the contact is a significant performance parameter.

Model overview

As outlined by Gupta *(13)*, there are basically two types of rolling bearing models used for rolling bearing performance simulation: *(1)* a static equilibrium model and *(2)* a generalized dynamics model.

Static equilibrium model

As shown schematically in Fig. 1, the fundamental input for all interactions is the relative position of the balls and races. Generally, the outer race mass center is fixed at the origin of a space fixed reference coordinate frame and the position vectors of the inner race and balls are defined relative to this reference frame. For a typical ball bearing with prescribed position of the balls and races, the equilibrium equations for ball and race are written as follows:

Ball equilibrium:

$$\text{Axial equilibrium}: \quad \sum_{j=1}^{2} Q_j \sin \alpha_j = 0 \qquad [1a]$$

$$\text{Radial equilibrium}: \quad \sum_{j=1}^{2} Q_j \cos \alpha_j - F_c = 0. \qquad [1b]$$

Here Q, α, and F_c are respectively the contact load, contact angle, and the applicable centrifugal force on the ball; the subscript j (equal to 1 or 2) is used to represent the outer and inner races, respectively. Both the contact loads and angles are a function of the relative axial (x) and radial (r) position of the ball mass center. The centrifugal force is computed in terms of ball mass, radial position, and orbital velocity, which is discussed later. The equations may be simultaneously solved for the ball axial and radial position (x, r).

Race equilibrium:

$$\text{Equilibrium along the } X \text{ axis}: \quad \sum_{i=1}^{N} Q_{2i} \sin \alpha_{2i} = Q_x \qquad [2a]$$

$$\text{Equilibrium along the } Y \text{ axis}: \quad \sum_{i=1}^{N} Q_{2i} \cos \alpha_{2i} \sin \psi_i = Q_y \qquad [2b]$$

$$\text{Equilibrium along the } Z \text{ axis}: \quad \sum_{i=1}^{N} Q_{2i} \cos \alpha_{2i} \cos \psi_i = Q_z. \qquad [2c]$$

Here ψ is the azimuth angle as defined in Fig. 1, and N is the number of balls in the bearing. These equations may be solved simultaneously to determine the relative inner race position (X, Y, Z).

Angular velocities

The ball angular velocity vector, ω, in an angular contact ball bearing is normally oriented at an angle, β, relative to the shaft axis, as also shown schematically in Fig. 1. Thus, the ball angular velocity may be defined by its two components along the x and z axes. The other unknown is the ball orbital velocity, $\dot{\theta}$, not shown in Fig. 1. For these three unknowns, the quasi-static models generally use the following three kinematic conditions:

1. Pure rolling at the center of the outer race contact.
2. Pure rolling at the center of the inner race contact.
3. An empirical race control hypothesis that permits relative ball spin only on the relatively lightly loaded race.

Pure rolling implies that the surface velocities on the ball and race are equal. Thus, conditions 1 and 2 are well defined. Condition 3 is empirical and was introduced by Jones *(1)*. The hypothesis states that relative spin, a component of ball angular velocity relative to the race about the load axis, normal to the ball–race contact surface, will exist only on the race that provides lesser of the spin moment. The race with no relative spin is called the controlling race. Assuming that the friction forces are proportional to the normal forces, Jones *(1, 2)* has expressed the race control hypothesis strictly in terms of the Hertzian pressure distribution over an elliptical contact. Therefore, although this simple hypothesis provides the required equation for computation of ball angular velocities, it does not implement any tribological behavior in the ball–race contact.

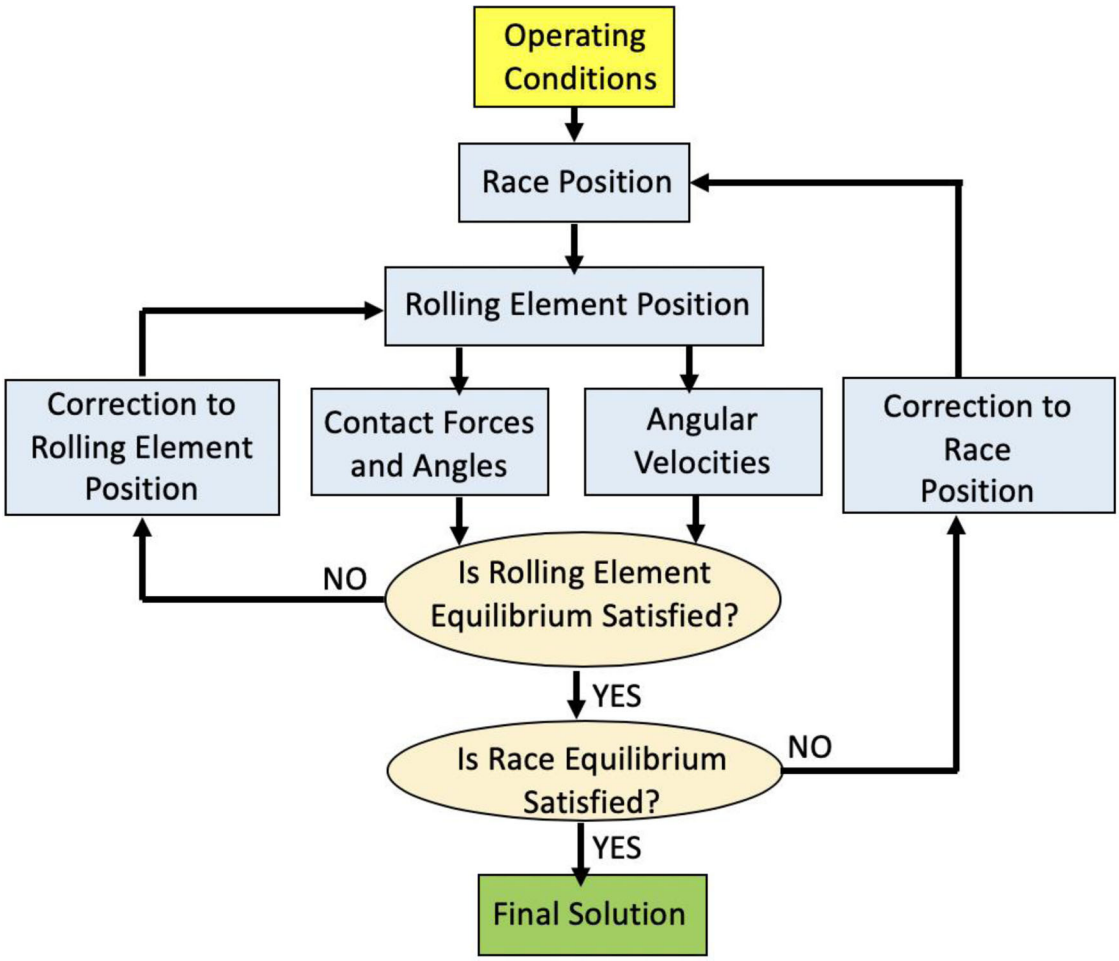

Figure 2. Schematic flowchart of quasi-static bearing performance model.

Model implementation

Because the relation between contact load and deflection is nonlinear in the commonly used Hertzian-type contact mechanics solution, implementation of the quasi-static model is an iterative process. As outlined in the flowchart in Fig. 2, for the prescribed operating conditions, the first step is to set the race at an initial position. The next step is to set the position of each ball. Ball–race interaction analysis is then carried out to compute contact loads and ball angular and orbital velocity components. The ball equilibrium Eqs. [1a] and [1b] are then checked and appropriate correction to the ball position is estimated, and the process is repeated with the corrected position until the ball equilibrium equations are satisfied. The process is repeated for each ball in the bearing. Once the ball equilibrium equations are satisfied, the contact loads are substituted in the race equilibrium Eqs. [2a]–[2c] and correction to the race position is estimated, and the process is repeated with the corrected race position until the race equilibrium is satisfied. Thus, as shown schematically in Fig. 2, there are two iterative loops: an outer loop for race equilibrium and the inner loop for ball equilibrium.

For a prescribed operating speed and applied load on the bearing, the above quasi-static model provides a detailed load distribution and contact stresses on the all the balls, which may be used for computing life and other commonly used bearing design parameters. However, the model is free of any tribological interaction at the ball–race contact.

Dynamic model

In the dynamic model the equilibrium equations are replaced by differential equations of motion. For any bearing element, as schematically shown in Fig. 3, the equations of motion in cylindrical coordinate frame, $(x,\ r,\ \theta)$, are written as follows:

Mass center motion in inertial frame:

$$m\ddot{x} = F_x \quad [3a]$$

$$m\ddot{r} - mr\dot{\theta}^2 = F_r \quad [3b]$$

$$mr\ddot{\theta} + 2m\dot{r}\dot{\theta} = F_\theta. \quad [3c]$$

Angular motion in body-fixed frame:

$$I_1\dot{\omega}_1 - (I_2 - I_3)\omega_2\omega_3 = M_1 \quad [4a]$$

$$I_2\dot{\omega}_2 - (I_3 - I_1)\omega_3\omega_1 = M_2 \quad [4b]$$

$$I_3\dot{\omega}_3 - (I_1 - I_2)\omega_1\omega_2 = M_3. \quad [4c]$$

The applied force vector in Eqs. [3a]–[3c] and the applied moment vector in Eqs. [4a]–[4c] contain all of the applied loads and moments, including those resulting from lubricant

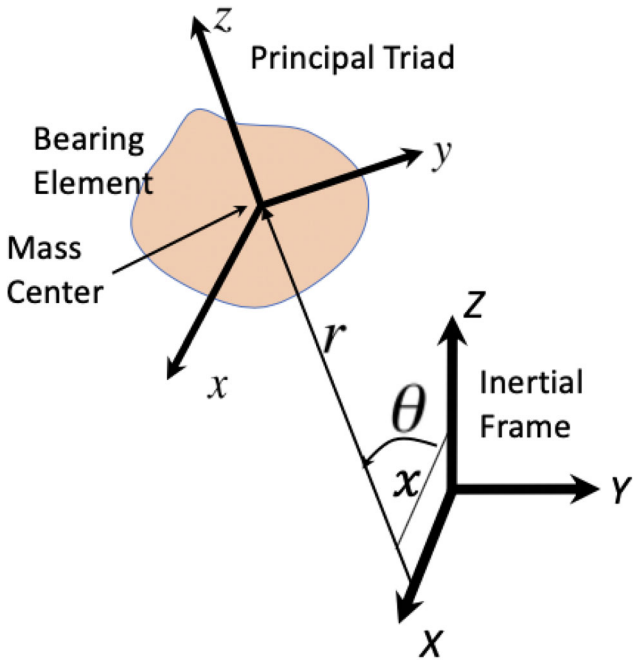

Figure 3. Base coordinate frame for differential equations of motion of bearing elements.

traction in the ball–race contacts. Thus, the model provides a complete interface with tribological behavior at the ball–race contacts. Note that the dynamic model replaces the algebraic equilibrium equations with differential equations of motion. Although no iterations are required in the dynamic model, the equations of motion have to be integrated in time with prescribed initial conditions until a steady-state behavior is reached. Normally, the quasi-static analysis is carried out to prescribe the initial conditions. The bearing dynamics code ADORE *(12)* is based on such a dynamic formulation.

Elastohydodynamic traction

The friction behavior or traction in concentrated contacts formed by ball–race interactions has been a subject of interest over the past several decades, and models with varying degrees of complexity are available to simulate traction as a function of slip rate in high-pressure concentrated ball–race contacts. Due to complexities associated with the measurement of lubricant rheology under high pressure, traditionally, lubricant traction has been measured in traction rigs and back-fitted to a model that could be used in bearing performance models. However, due to operating limits of most traction rigs, the experimentally measured traction behavior has to be extensively extrapolated to operating conditions in the bearing, which are often greatly different from the conditions used in most traction rigs. This results in significant uncertainties in the prediction of bearing performance. Fortunately, with the recent advances in high-pressure viscometers (9), traction prediction, based on independently measured lubricant behavior, has now become possible *(22)*. With reference to the contact schematic shown in Fig. 4, the model is simply formulated in terms of the following fundamental equations:

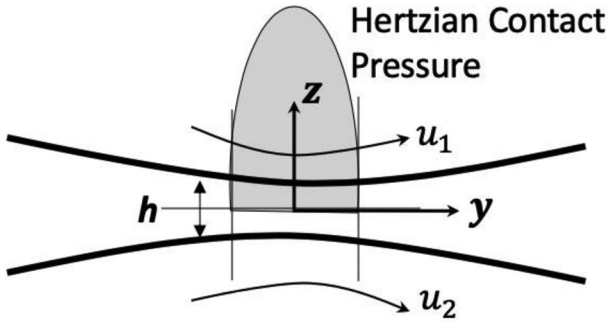

Figure 4. Schematic of an elastohydrodynamic contact.

$$\text{Energy equation:}\quad K(p,T)\frac{\partial^2 T}{\partial z^2} = -\tau\dot{\gamma} \qquad [5a]$$

$$\text{Geometric compatibility:}\quad \frac{\partial u}{\partial z} = \dot{\gamma}(\tau,p,T) \qquad [5b]$$

$$\text{Constitutive equation:}\quad \dot{\gamma}(\tau,p,T) = \frac{\tau}{\mu(p,T)}. \qquad [5c]$$

Here μ and K are respectively the lubricant viscosity and thermal conductivity, both dependent on pressure, p, and temperature, T; τ and $\dot{\gamma}$ are respectively the shear stress and strain rate; u is the fluid velocity; and z is the coordinate through the lubricant film.

As shown by Gupta et al. *(22)*, a simultaneous integration of the above equations in a ball–race contact provides the Newtonian shear stress, τ, over the contact. The model does not include surface finish and any role of partial elastohydrodynamic lubrication or boundary films. Likewise, there are no starvation effects and the ball–race contact is assumed to have full film lubrication. Recent advances in high-pressure lubricant rheology *(9)* have shown that lubricant viscosity, in addition to pressure and temperature, may also depend on shear stress. The effect is called "shear-thinning". The computed Newtonian traction, by simultaneous solutions of Eqs. [5a]–[5c], may be corrected to allow for the shear-thinning effects as

$$\overline{\tau} = \tau\left[1 + \left(\frac{\tau}{G}\right)^2\right]^{\frac{n-1}{2}}, \qquad [6]$$

where $\overline{\tau}$ is the effective shear stress, τ is the Newtonian shear stress, G is an effective shear modulus, and n is a shear-thinning exponent. As shown by Gupta et al. *(22)*, the above approach provides traction predictions that are in good agreement with experimental data. The model is therefore implemented in the bearing dynamics computer code ADORE *(12)*. In addition to the dynamic simulation, this model is used in the present investigation to incorporate elastohydrodynamic traction effects in quasi-static equilibrium solution.

Minimum energy hypothesis for quasi-static bearing model

As reviewed above, the presently used quasi-static bearing model does not provide a realistic interaction with lubricant traction in ball–race contacts. Instead, kinematic conditions are used to apply pure rolling in the center of ball–race

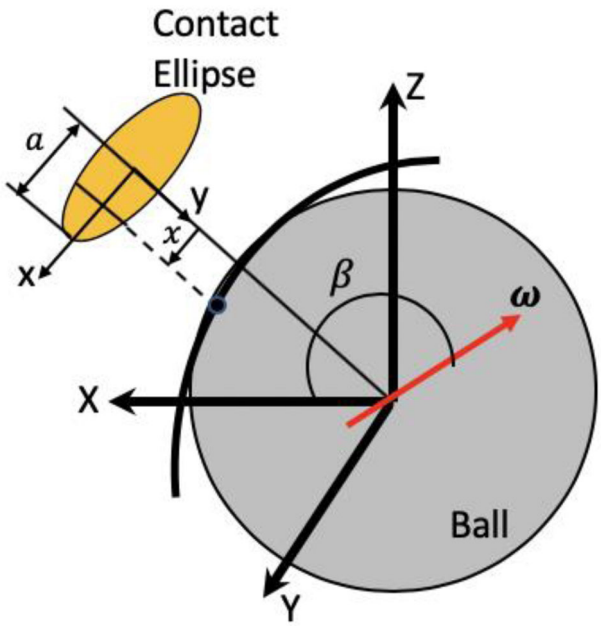

Figure 5. Exaggerated outline of ball–race contact.

contacts and an empirical race control hypothesis is used to restrict relative ball spin to only one of the races, which has a relatively lower spin torque. Furthermore, with the assumption of a constant friction coefficient, the spin torque is expressed only in terms of the contact load over the elliptical contact area. These three conditions permit computation of the three unknowns; that is, two components of ball angular velocity and the ball orbital velocity as it travels around the bearing.

A more in-depth review of the ball–race contact, as shown schematically in Fig. 5, reveals that because the ball–race contact is on a curved surface with an effective radius, defined by the curvature of interacting ball and race surfaces, the slip velocity varies along the major axis of the contact ellipse. The slip distribution depends on the location of the point of pure rolling, as illustrated schematically by Anderson *(16)*. When the applicable traction is related to slip, the frictional dissipation, or the energy dissipated in the contact depends on the location of point of pure rolling in the contact and the prescribed orientation of the ball angular velocity vector, β. In general, with a prescribed lubricant traction model, the three independent variables, which permit computation of the frictional dissipation, are the pure rolling points in the outer and inner race contacts, x_1, x_2 respectively, and the orientation of ball angular velocity vector, β, as shown in Figs. 1 and 5.

In the proposed minimum energy hypothesis, the total frictional dissipation, q, is minimized as a function of these three independent variables. Thus, the total dissipation is written as

$$q = q(x_1, x_2, \beta) = q_1(x_1, x_2, \beta) + q_2(x_1, x_2, \beta), \qquad [7]$$

where q_1 and q_2 are the dissipations in the outer and inner race contacts respectively.

Table 1. Ball bearing geometry.

Bearing bore	120 mm	Pitch diameter	155 mm
Bearing outer diameter	190 mm	Contact angle	24°
Number of balls	15	Outer race curvature factor	0.52
Ball diameter	20.6375 mm	Inner race curvature factor	0.54

For the total dissipation to be minimum,

$$\frac{\partial q}{\partial x_1} = 0 \qquad [8a]$$

$$\frac{\partial q}{\partial x_2} = 0 \qquad [8b]$$

$$\frac{\partial q}{\partial \beta} = 0. \qquad [8c]$$

For a prescribed bearing geometry, operating conditions, and the applicable lubricant traction model, Eqs. [8a] to [8c] are solved to compute the ball angular and orbital velocities in the bearing. The model is implemented as a modification to the quasi-static module in the widely distributed bearing dynamics code ADORE *(12)*.

Test bearing and model implementation

Model implementation is best illustrated by its application to a test bearing. Thus, a typical high-speed turbine engine is used to demonstrate model significance and its implementation. The bearing geometry is summarized in Table 1.

The bearing material is M-50 VIMVAR bearing steel and the lubricant is the commonly used MIL-L-23699 jet oil , for which a validated traction model is available in the recent work by Gupta et al. *(22)*. The bearing operates at a speed of 25,000 rpm (3 million DN) with a thrust load of 22,240 N (5,000 lbf) at an operating temperature of 492 K. The selection of this particular lubricant and operating conditions, including the operating temperature, is quite arbitrary. The purpose is simply to demonstrate the model significance in a prescribed operating environment.

In high-speed ball bearings, very often the ball riding over the inner race shoulder is a common problem. However, the factors that control such a behavior are the ball centrifugal force and the operating inner race contact angle, which is related to the initial internal clearance, centrifugal expansion of the rotating inner race, initial shrink fits on the bearing, and the thermal expansion of bearing races as a function of operating temperature. Although the ball velocities as computed in the minimum energy hypothesis are different from those computed with the commonly used race control theory, the differences are only significant for computation of frictional dissipations, and they are too small to influence the contact angles and over all contact configuration. It should also be noted that the energy dissipation in the present investigation only consists of frictional dissipation in ball–race contacts. Any lubricant churning and drag effects, which are major contributors to overall bearing heat generation, are excluded. Likewise, in order to emphasize the ball–race contact dissipation, the bearing is cageless and there are no cage contacts.

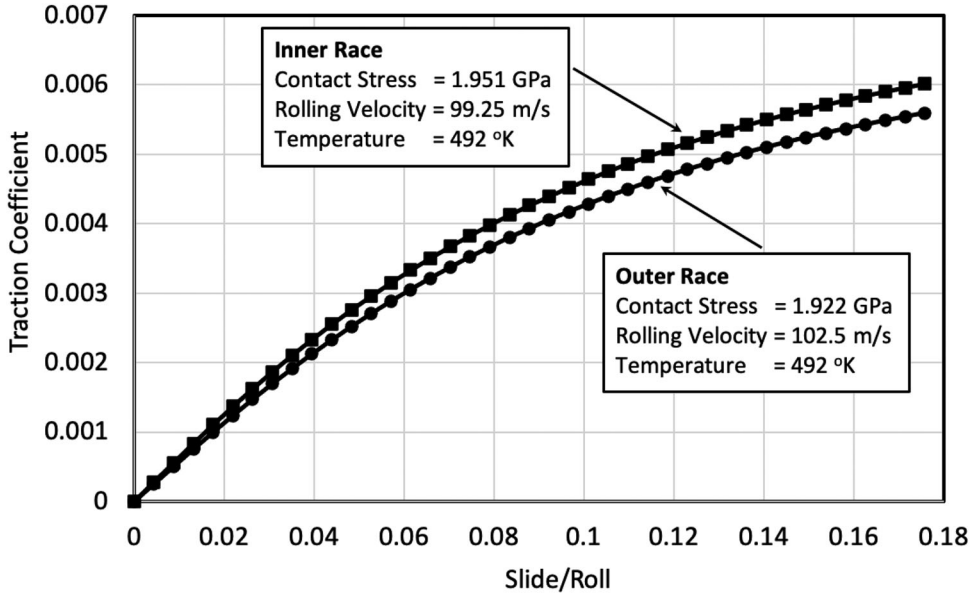

Figure 6. Applicable traction curve for the MIL-L-23699 lubricant under the prescribed operating conditions for the 120-mm high-speed ball bearing.

Under the above operating conditions, the elastohydrodynamic traction model with shear-thinning effects provides the traction–slip relations shown in Fig. 6. These relationships are used to generate the frictional dissipation in the contact. Though the values of traction coefficients appear to be low in Fig. 6, the values are computed from an experimentally validated traction model *(22)*, as discussed above. In any case, the present use of these data as input to the model is only an example to demonstrate model functionality.

Corresponding to Eqs. [8a] to [8c], model implementation is a three-step process. First, for prescribed value of the angular velocity vector orientation, β, and the point of pure rolling in the outer race contact, x_1, the point of pure rolling in the inner race contact, x_2, is varied to obtain minimum total dissipation. For the test bearing presented above, with the prescribed ball angular velocity vector orientation and the rolling point on the outer race, the total dissipation as a function of pure rolling point in the inner race contact, x_2, is shown in Fig. 7.

The entire contact length is first scanned for the total dissipation to determine the vicinity of the minimum dissipation point. The data are then fitted to a parabolic variation and the point at which the partial derivative of total dissipation is zero is determined.

$$\frac{\partial q(x_1, x_2, \beta)}{\partial x_2} = 0 \qquad [9a]$$

at

$$x_2 = x_{21m\beta} = x_{21m\beta}(x_1, \beta). \qquad [9b]$$

Corresponding to this minimum dissipation point, the minimum dissipation is determined as a function of pure rolling point on the outer race and orientation of the ball angular velocity vector:

$$q_{m1\beta} = q_{m1\beta}(x_1, \beta). \qquad [10]$$

In the second step the dissipation computed in Eq. [10] is scanned over the length of the outer race contact to determine the minimum dissipation point on the outer race using the procedure discussed above for the inner race. Thus, at the minimum dissipation point on the outer race,

$$\frac{\partial q_{m1\beta}(x_1, \beta)}{\partial x_1} = 0 \qquad [11a]$$

at

$$x_1 = x_{1m\beta} = x_{1m\beta}(\beta). \qquad [11b]$$

The corresponding minimum dissipation is

$$q_{m\beta} = q_{m\beta}(\beta). \qquad [12]$$

Equations [9b] and [11b] may now be combined to obtain the final point of pure rolling in the inner race contact:

$$x_{2m\beta} = x_{2m\beta}(\beta) = x_{21m\beta}(x_{21m\beta}, \beta). \qquad [13]$$

The total dissipation, as computed by Eq. [12], and the applicable inner race coordinate, as computed by Eq. [13], for the test bearing, are plotted in Fig. 8 as a function of the outer race coordinate. It is interesting to note that variation in the point of pure rolling on the inner race is qualitatively an inverse mirror image of the variation in the total dissipation. Again, the data are fitted to a parabolic variation in the vicinity of the minimum dissipation point to determine the point of minimum dissipation and the applicable rolling point on the inner race.

In the final step, the minimum dissipation computed in Eq. [12] is scanned over a range of values of β to determine the final value of minimum dissipation, the corresponding orientation of ball angular velocity vector, and the points of pure rolling in the outer and inner race contacts:

$$\frac{\partial q_{m\beta}}{\partial \beta} = 0 \qquad [14a]$$

at

$$\beta = \beta_m. \qquad [14b]$$

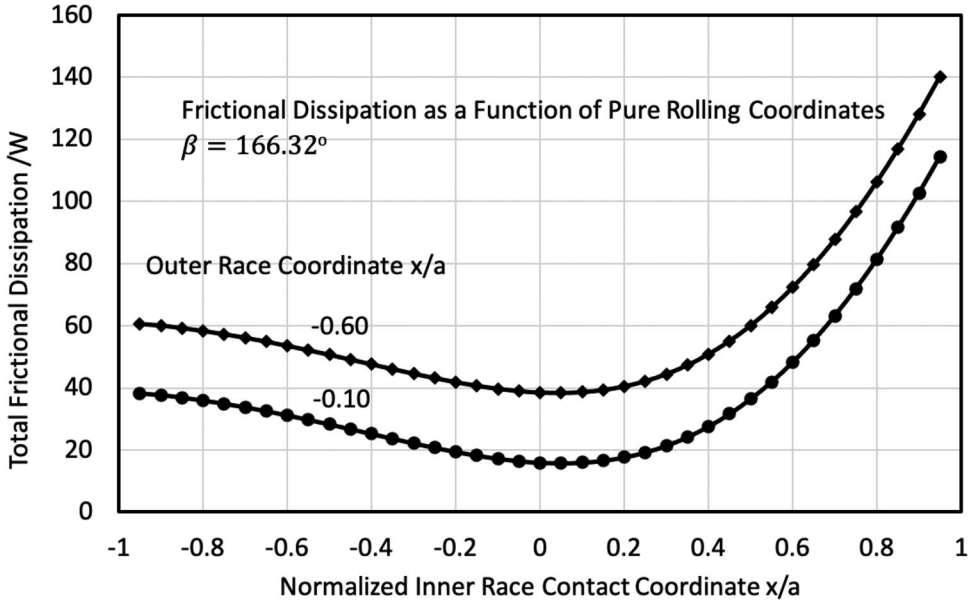

Figure 7. Variation in the sum of frictional dissipation in outer and inner race contacts for an individual ball as a function of pure rolling point in the inner race contact at a prescribed orientation of ball angular velocity vector and rolling point in the outer race contact.

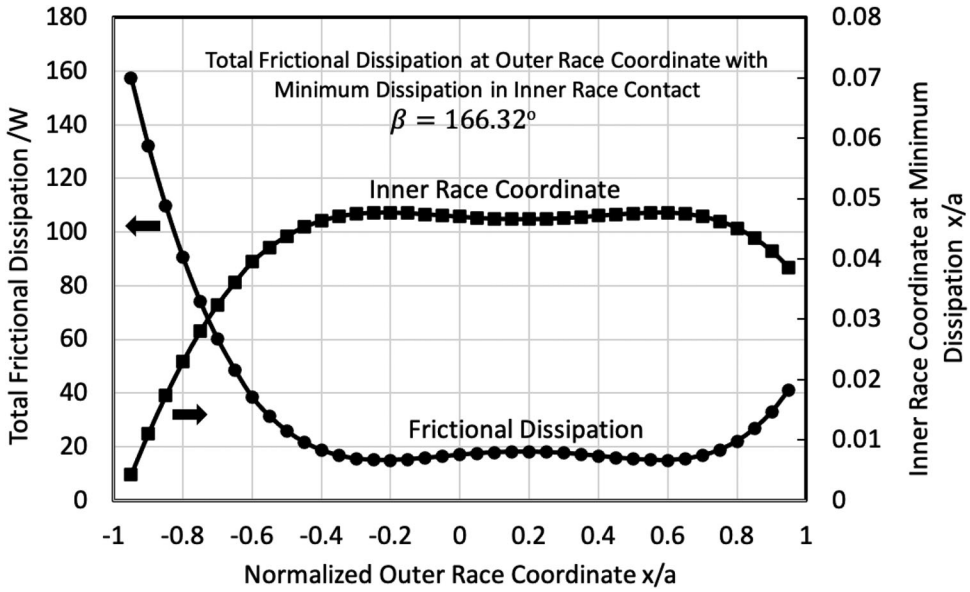

Figure 8. Total minimum contact dissipation for an individual ball and the applicable pure rolling point in the inner race contact plotted as a function of rolling point in the outer race contact.

The corresponding dissipation is the minimum dissipation

$$q = q_m. \quad [15]$$

The total dissipation as a function of the ball angular velocity vector orientation for the test bearing is shown in Fig. 9.

The data are once again fitted to a parabolic variation in the vicinity of minium point to determine the final value of the minimum dissipation point.

A schematic representation of the overall implementation process is presented in Fig. 10. The three steps in the model implementation process are clearly outlined.

It should be noted that the traction model is called at each computation of contact dissipation. Therefore, depending on the complexity of the traction model, the process may be computationally intensive. However, the overall computing effort is still quite small in comparison to that required for dynamic simulations over several shaft revolutions. The contact parameters computed from the contact mechanics model are held constant during the dissipation minimization process. This is quite reasonable because a very small change in the ball orbital velocity is insignificant in terms of the change in centrifugal force, and it does not alter the force equilibrium to any notable extent. Implementation of the hypothesis in the quasi-static equilibrium model is accomplished by replacing the angular velocity computation box in Fig. 2 by the minimum energy model shown in Fig. 10. It is also found that when the initial solution in the contact dissipation minimization process is set by the race control hypothesis, only a limited range of contact area has to be scanned to determine the minimum

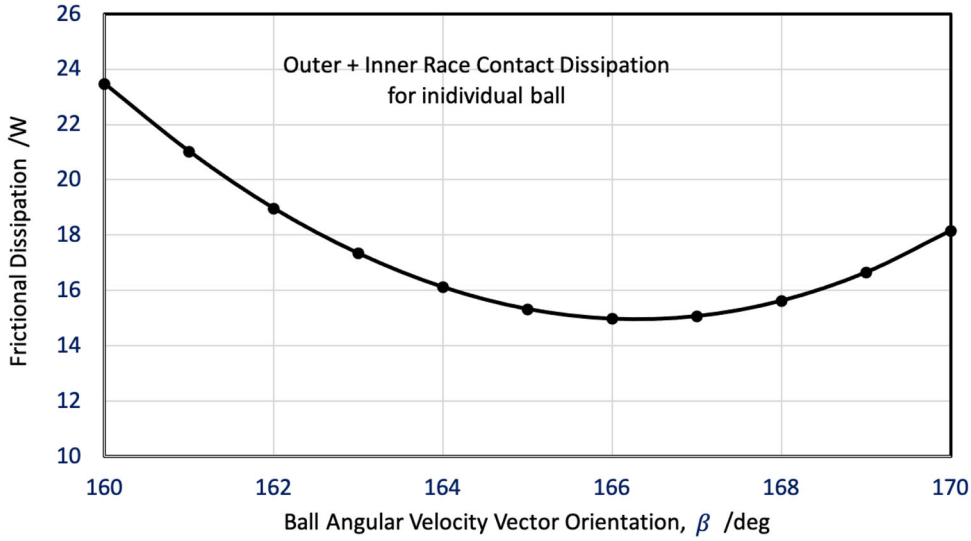

Figure 9. Total contact dissipation for an individual ball as a function of the ball angular velocity vector in the test bearing.

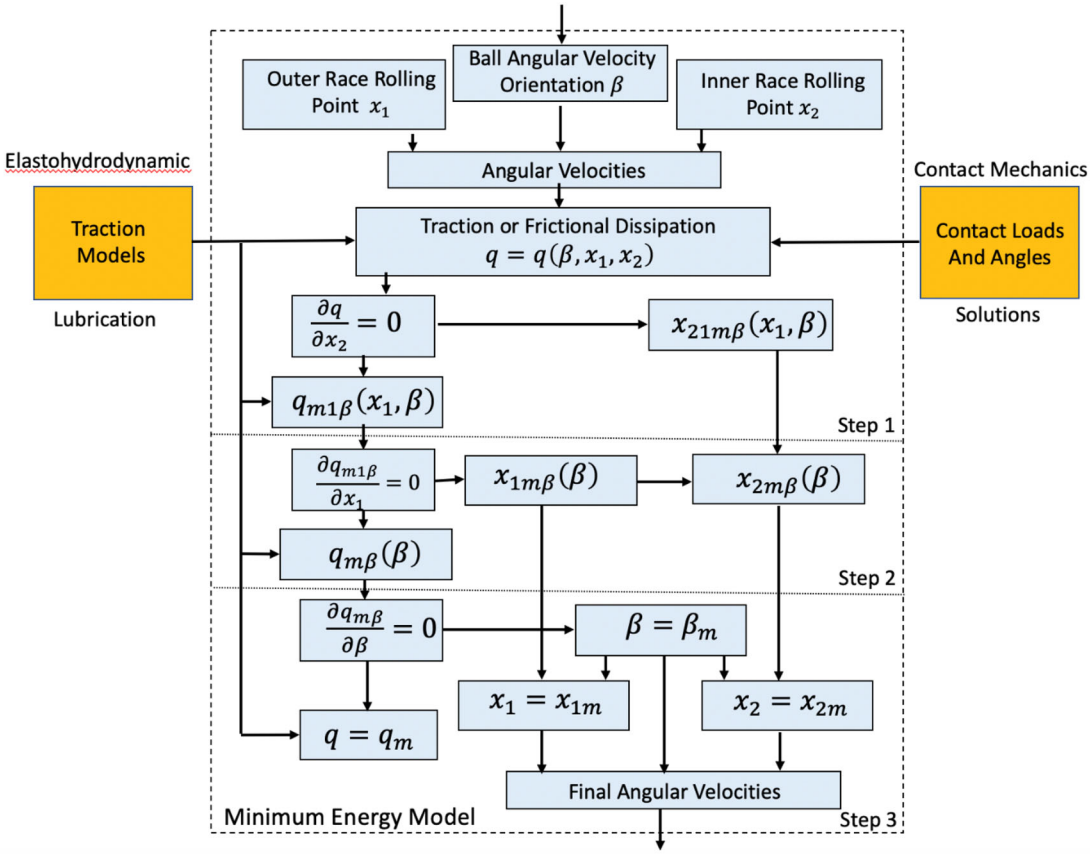

Figure 10. Implementation of the minimum energy hypothesis for computing the ball angular velocity in a quasi-static model for a ball bearing.

contact dissipation. This leads to a notable improvement in the overall computational efficiency.

Comparison of quasi-static and steady-state dynamic solutions

The above enhancement is implemented in the quasi-static module in the bearing dynamics code ADORE *(12)*, and both the quasi-static and fully dynamic solutions are obtained for the test bearing to test the practical significance of the proposed minimum energy hypothesis for the quasi-static solution. In the dynamic runs, where the simulations are carried out over several bearing revolutions, there are no ball-to-ball collisions, although the bearing is cageless. Because the bearing is thrust loaded, all motion parameters for all the balls are identical; therefore, the spacing between balls remains unchanged throughout the simulations.

Under the race control hypothesis introduced by Jones *(1, 2)*, the bearing is outer race controlled. This implies that

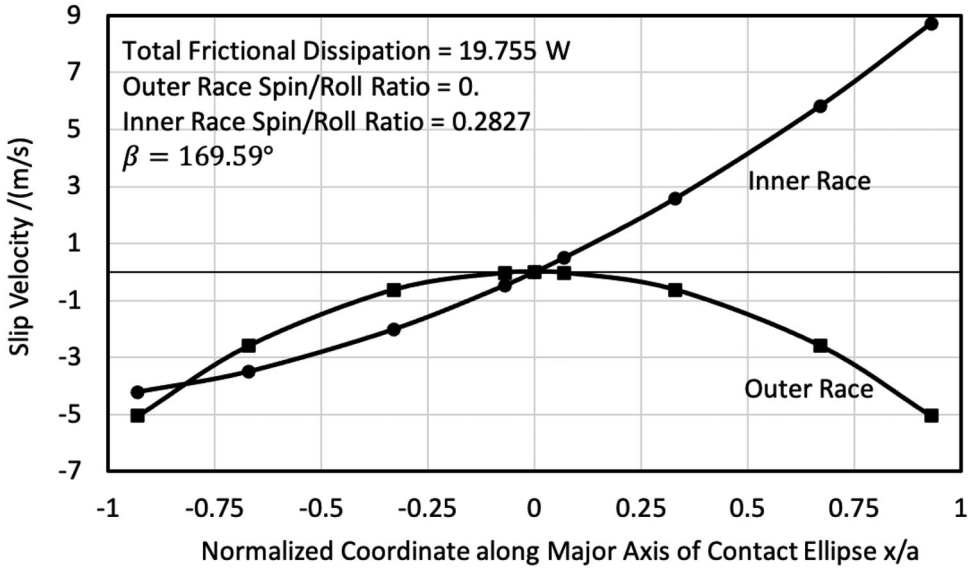

Figure 11. Ball–race slip velocity distribution under the outer race control hypothesis.

all relative spin is restricted to the inner race contact. The resulting slip velocity distributions in the contact are shown in Fig. 11. The sum of frictional dissipation at the outer and inner race contacts under the traction–slip behavior shown in Fig. 6, orientation of ball angular velocity, and the resulting spin-to-roll ratios at the outer and inner race contacts are also documented in Fig. 11. Note that corresponding to outer race control, the spin-to-roll ratio on the outer race is zero. The points of pure rolling on both the outer and inner race contacts are in the center of the contact. The ball orbital and angular velocities are computed from kinematic conditions and the empirical race control hypothesis as discussed above. Lubricant traction behavior has no input in these computations. Once the velocities are determined, the traction behavior is used to compute the frictional dissipation in the contact.

When the points of pure rolling on the outer and inner races are varied to minimize the sum of frictional dissipation at the outer and inner race contacts, the orientation of the ball angular velocity vector is altered and the slip distribution changes. In the process, the quasi-static model is completely interfaced with the traction behavior shown in Fig. 6. The resulting slip distributions under minimum frictional dissipation are shown in Fig. 12. Note that the pure rolling point on the inner race has moved slightly to the right of contact center, which implies a combination of rolling and spinning in the contact. On the outer race, there are now two points of pure rolling that are not symmetric about center of the contact. This also implies both rolling and spinning in the contact. Thus, the spin-to-roll ratios are non-zero on both races. When compared to the outer race control solution in Fig. 11, although the change in orientation of ball angular velocity vector is small, the frictional dissipation is about 24% less. This reduction is, of course, dependent on the traction behavior in the contact. It should also be noted that when there are two points of point rolling, the ball angular velocity is completely defined by any one of the two points. Thus, it is only necessary to scan for one of the rolling points during the model implementation process, discussed above.

The next step is to generate a fully dynamic simulation and compare the steady-state solution with the quasi-static solution with minimum frictional dissipation. For this purpose, ADORE is executed in the dynamic mode with the quasi-static solution as the initial condition. In order to eliminate the very high-frequency ball-to-race contact vibration and substantially increase the permissible time step, the ball mass center is constrained to meet the force equilibrium equation, and the differential equations of ball angular and orbital motion are integrated in the time domain. As the solution reaches a dynamic steady state, all accelerations introduced by arbitrarily selected initial conditions are eliminated and the bearing reaches a true dynamic steady-state behavior. The simulation is run over 400 shaft revolutions so that the steady-state condition is very well defined. To demonstrate the practical significance of the proposed minimum energy hypothesis, two dynamic simulations are obtained, one with the initial condition set by the quasi-static solution with minimum energy hypothesis and the other with the commonly used race control, as introduced by Jones *(1, 2)*. The slip distribution solutions under dynamic steady-state conditions, with a quasi-static solution with minimum energy hypothesis as initial condition, are plotted in Fig. 13. Note the closeness of these distributions with those shown in Fig. 12 for the quasi-static solution, which is used as initial condition in the dynamic simulation. Differences between the total frictional dissipation, slide-to-roll ratios, and orientation of the ball angular velocity vector are insignificant. The points of pure rolling in the two solutions are also quite close to each other.

The slip distribution solutions corresponding to the dynamic steady state obtained with the quasi-static solution, with the race control hypothesis as the initial condition, are presented in Fig. 14. Clearly, these solutions are also quite close to the steady-state solutions shown in Fig. 13 and the

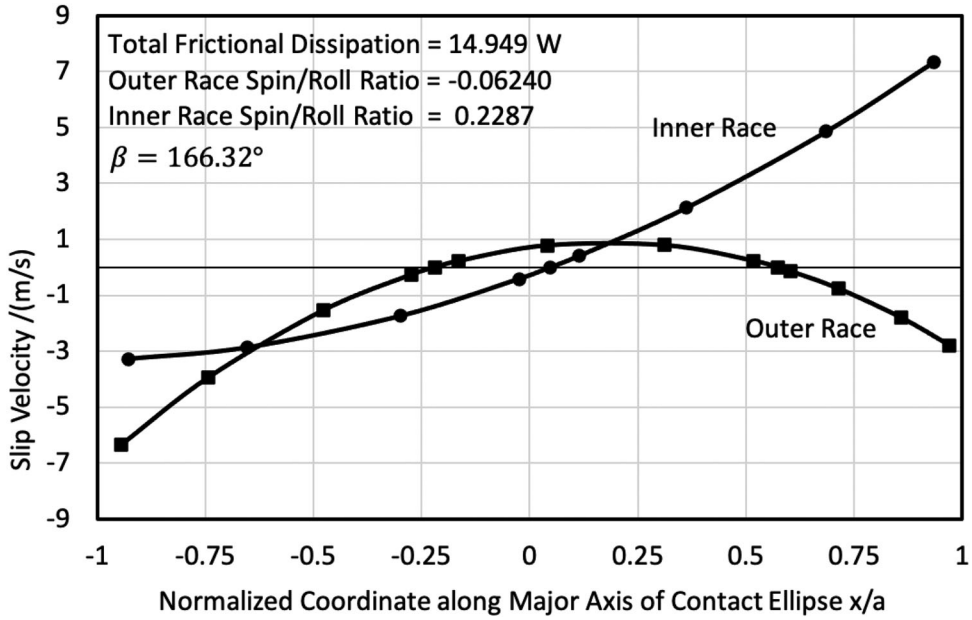

Figure 12. Ball–race slip distribution in quasi-static solution under the minimum energy hypothesis.

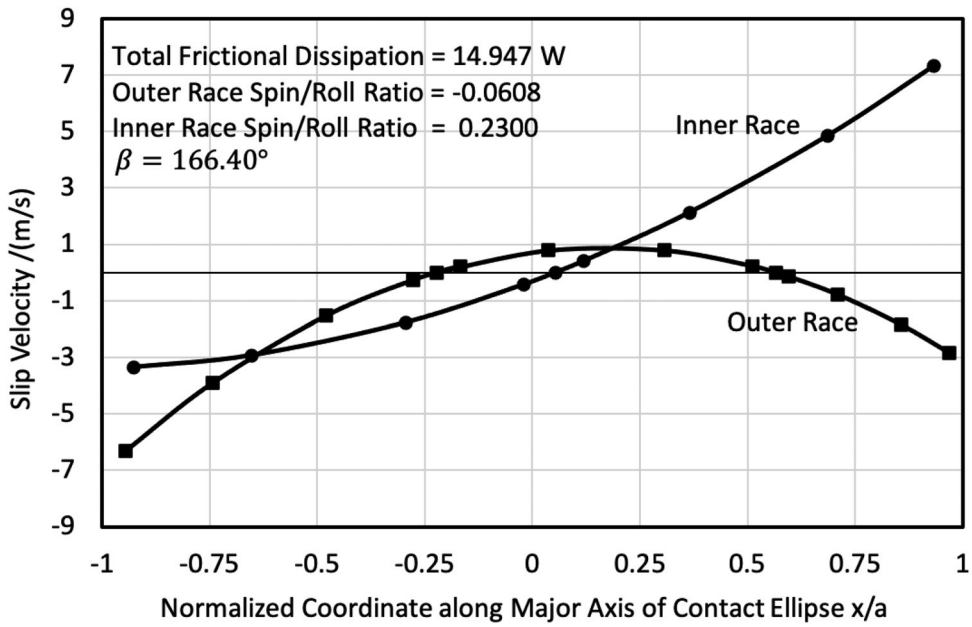

Figure 13. Ball–race slip distribution in the steady-state solution obtained with a fully dynamic analysis with the quasi-static solution based on the minimum energy hypothesis as the initial condition.

quasi-static solutions with the minimum energy hypothesis in Fig. 12.

The closeness between the quasi-static solution obtained with the minimum energy hypothesis and fully dynamic steady-state solution may be further demonstrated by the dynamic solution shown in Figs. 15a and 15b, where the spin-to-roll ratios for the outer and inner races are respectively plotted in the time domain. The initial conditions for these solutions are defined by the quasi-static solution with the minimum energy and race control hypotheses. Note that there is practically no difference in the spin-to-roll ratios between the initial condition and the final dynamic steady-state when the minimum energy hypothesis is used as the initial condition. When the initial conditions are set by the race control hypothesis, the solutions converge to those obtained with the minimum energy hypothesis as the bearing reaches a steady-state.

The frictional dissipation or the total energy dissipated in the outer and inner race contacts is shown in Fig. 16. Though the dynamic steady-state solution remains relatively unchanged from the initial condition set by the minimum energy hypothesis, the contact dissipation rapidly falls from the race control value to the value obtained by the minimum energy hypothesis as the bearing reaches a steady-state with the outer race control solution as initial condition. These comparisons lead to the conclusion that the quasi-static solution with the minimum energy hypothesis can provide a more realistic estimate of frictional dissipation, or

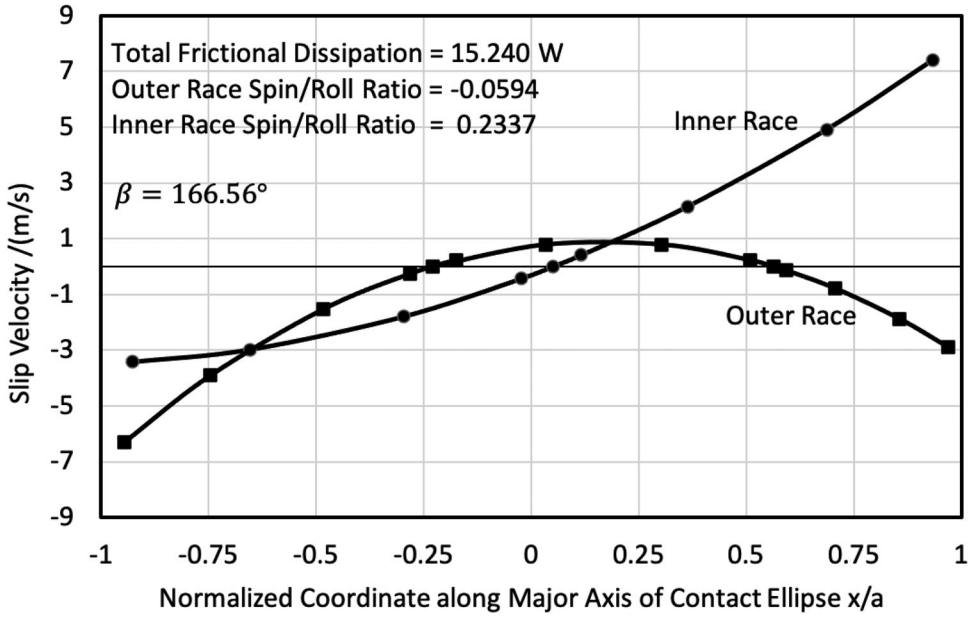

Figure 14. Ball–race slip distribution in the steady-state solution obtained with a fully dynamic analysis with the quasi-static solution based on the race control hypothesis as the initial condition.

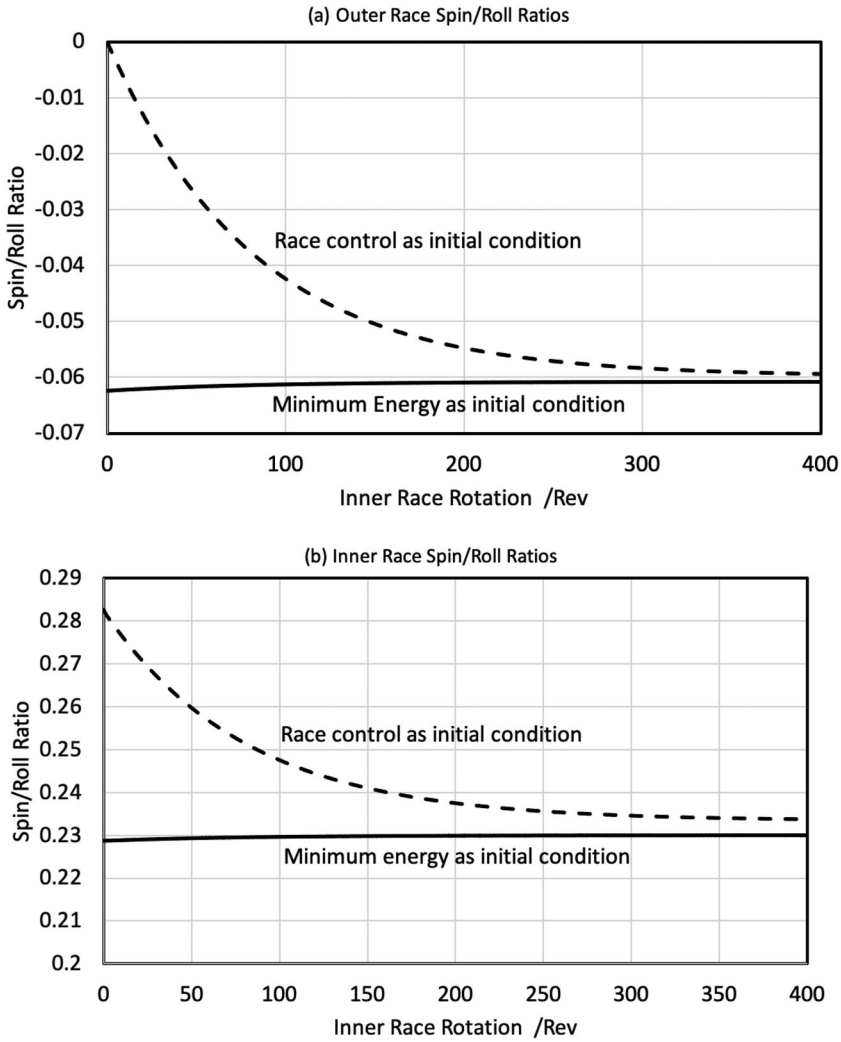

Figure 15. Time domain dynamic solutions for spin-to-roll ratios with the quasi-static solutions based on minimum energy and race control hypotheses as initial conditions.

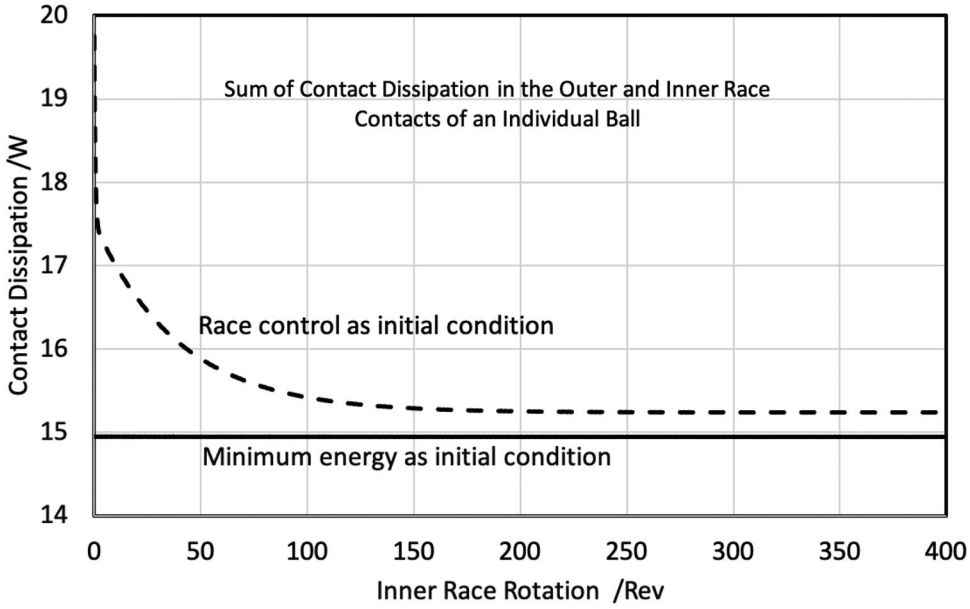

Figure 16. Comparison of dynamic solutions of total frictional dissipation in the outer and inner race contacts obtained with quasi-static solutions based on minimum energy and race control hypotheses as initial conditions.

heat generation, in ball–race contacts. Such a finding is significant for practical bearing design purposes, particularly for parametric evaluation of hybrid bearings when the steel rolling elements are replaced by silicon nitride elements in the hopes of improved contact heat generation and overall bearing performance.

In dynamic simulations obtained by integration of differential equations of motion, the steady-state solutions under prescribed operating conditions do not depend on initial conditions when the integration process is stable. However, in the solutions presented above with two different initial conditions, the steady-state solutions show a small difference, although the difference is insignificant. It turns out that the contact loads and angles, which are held fixed during the integration of differential equations of motion, are slightly different in the quasi-static solutions obtained by the minimum energy and race control hypotheses. This is noted when the solutions are compared in more detail. This comparison is provided in Table 2, where the contact parameters are summarized in more detail. It is noted that the equilibrium solutions with race control and minimum energy hypotheses are not numerically identical. The small difference in the two dynamic steady-state solutions is correlated to this slight difference in loads, angles, and other related contact parameters.

As an alternate comparison, the frictional dissipation provided by the various solutions may be displayed on a plot containing the minimum energy solution as a function of prescribed orientation of the ball angular velocity vector, β. This is done in Fig. 17, where the quasi-static solution points with minimum energy and race control hypotheses are also displayed along with the dynamic steady-state solution. Clearly, in terms of frictional dissipation, the dynamic steady-state and the quasi-static solutions with the minimum energy hypothesis are identical.

Because the proposed minimum energy hypothesis better defines the slip distribution in ball-to-race contacts, incorporation of the minimum energy hypothesis in the quasi-static bearing model may also provide more reliable prediction of wear in ball-to-race contacts, when the wear model is based on the load * slip (QV) integral over the race contacts. The slip distribution in the contact does contribute to this load * slip integral. Thus, improvement in load * slip estimates may lead to improved wear prediction. The sum of the load * slip (QV) integral over the outer and inner race contacts is plotted as a function of the orientation of the ball angular velocity vector in Fig. 18. Again, the solution points corresponding to the commonly used quasi-static model with the race control hypothesis, the quasi-static solution with the minimum energy hypothesis, and the dynamic steady-state solution are also displayed. Clearly, the quasi-static solution based on the minimum energy hypothesis and the dynamic steady-state solution are identical. Thus, the enhanced quasi-static model with the incorporation of tribological behavior at the ball–race contacts and implementation of the minimum energy hypothesis may also be valuable for wear prediction in rolling bearings. However, it must be emphasized that many other chemical and mechanical elements control wear prediction. For example, surface finish, lubricant adsorption at the contact surfaces, additives in the lubricant, lubricant film thickness, operating environment, etc., all are significant parameters in wear prediction. The load * slip integral as computed in the present example is only one element and is commonly used in Archard-type wear equations.

Implementation of the proposed minimum energy hypothesis in the quasi-static module in ADORE is indeed a fairly complex task. However, along with the common design parameters, such as bearing fatigue life, overall load distribution, lubricant film thickness, and bearing stiffness,

Table 2. Comparison of contact parameters in the various solutions.

	Quasistatic		Dynamic steady-state	
Parameter	Race control	Minimum energy	Race control initial condition	Minimum energy initial condition
Outer race contact load (kN)	7.257	7.191	7.257	7.191
Inner race contact load (kN)	3.525	3.533	3.525	3.533
Outer race contact angle (°)	11.79	11.90	11.79	11.90
Inner race contact angle (°)	24.87	24.81	24.87	24.81
Centrifugal force (kN)	3.906	3.830	3.835	3.832
Outer race contact stress (GPa)	1.922	1.916	1.922	1.916
Inner race contact stress (GPa)	1.951	1.952	1.951	1.952
Ball angular velocity (krpm)	94.63	94.38	94.46	94.41
Angle velocity vector orientation (°)	169.59	166.32	166.56	166.40
Ball orbital velocity (krpm)	11.14	11.03	11.03	11.03
Outer race spin–roll ratio	0	−0.0624	−0.0594	−0.0608
Inner race spin–roll ratio	0.2827	0.2287	0.2337	0.2300
Outer race frictional dissipation (W)	5.5907	5.3426	5.3018	5.2417
Inner race frictional dissipation (W)	14.164	9.6063	9.9383	9.705
Total frictional dissipation (W)	19.755	14.949	15.24	14.947

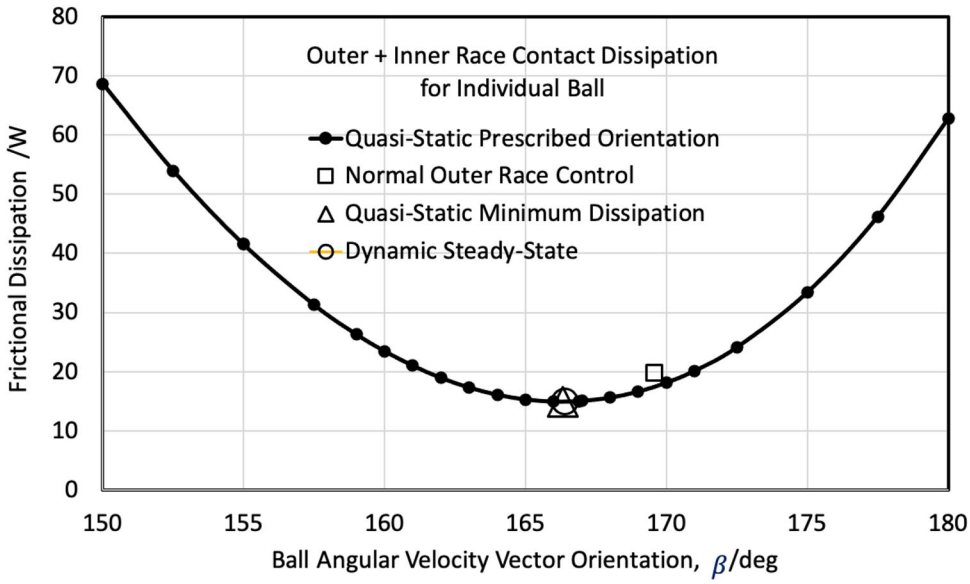

Figure 17. Frictional dissipation in ball-to-race contacts as a function of ball angular velocity vector orientation.

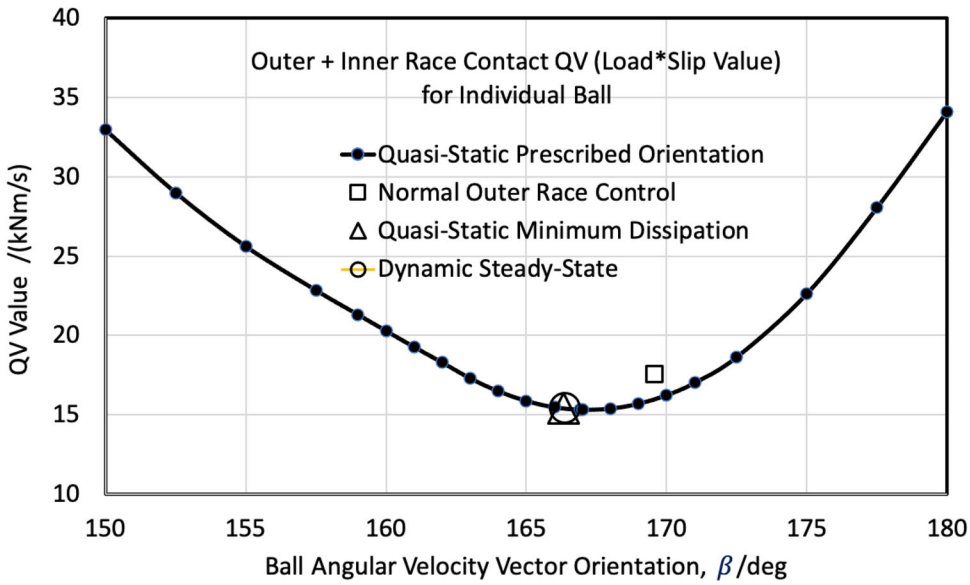

Figure 18. Integrated QV (load * slip) value as a function of orientation of the ball angular velocity vector as obtained by quasi-static solutions with the implementation of the minimum energy hypothesis.

the enhanced model provides realistic estimate of frictional dissipation, or heat generation, in the ball–race contact under a prescribed lubricant traction model. Thus, the enhanced quasi-static module in ADORE has a stand-alone significance for bearing design. It is therefore extracted from ADORE, packaged in a stand-alone application AdoreQS, and made freely available in the public domain *(23)*. The package, of course, includes the lubricant traction module, as required for implementation of the minimum energy hypothesis. It is hoped that this access to the computer code will facilitate immediate evaluation and practical implementation of the work reported in this article.

Summary

A proper integration of tribological behavior at ball–race interactions, contact mechanics, and dynamics is essential for realistic simulation of bearing performance. The present investigation enhances the widely used quasi-static bearing model by introducing a minimum energy hypothesis in place of the commonly used race control hypothesis. Unlike the race control hypothesis, the newly introduced minimum energy hypothesis provides a close coupling between the contact mechanics, bearing kinematics, and ball–race lubrication or traction model. It is shown that frictional dissipation or heat generation in ball-to-race contacts provided by the quasi-static solution with the minimum energy hypothesis is very close to that obtained by the significantly more sophisticated dynamic steady-state solution obtained by time domain integration of differential equations of ball motion. The improved prediction of ball–race slip also provides a meaningful estimate of load * slip values, which are used in wear prediction in ball–race contacts. Because realistic modeling of frictional dissipation in ball–race contacts is particularly significant in hybrid ball bearings, the quasi-static model with implementation of the proposed minimum energy hypothesis may provide an effective design tool for preliminary optimization of contact heat generation before undertaking a more detailed dynamics modeling.

References

(1) Jones, A. B. (1959), "Ball Motion and Sliding Friction in Ball Bearings," *Journal of Basic Engineering*, **81**, pp 1–12. doi:10.1115/1.4008346

(2) Jones, A. B. (1960), "A General Theory of Elastically Constrained Ball and Roller Bearings under Arbitrary Load and Speed Conditions," *Journal of Basic Engineering*, **82**, pp 309–320. doi:10.1115/1.3662587

(3) Harris, T. A. (1966), *Rolling Bearing Analysis*, John Wiley.

(4) Rumbarger, J. H., Filetti, E. G., and Gubernick, D. (1973), "Gas Turbine Engine Main Shaft Roller Bearing System Analysis," *Journal of Lubrication Technology*, **95**, pp 401–416. doi:10.1115/1.3451843

(5) Schlichtig, H. (1968), *Boundary Layer Theory*, McGraw Hill.

(6) Crecelius, W. J. and Pirvics, J. (1976), "Computer Program Operation Manual on SHABERTH: A Computer Program for the Analysis of the Steady-State and Transient Thermal Performance of Shaft Bearing System," **U.S. Air Force Technical Report AFAPL-TR-76-90**.

(7) Poplawski, J. V. *Computer Code COBRA*, J. V. Poplawski & Associates: Bethlehem, PA. Available at: http://www.bearingspecialists.com (accessed April 15, 2020).

(8) Hamrock, B. J. and Dowson, D. (1981), *Ball Bearing Lubrication: The Elastohydrodynamic Lubrication of Elliptical Contacts*, John Wiley & Sons.

(9) Bair, S. (2019), *High Pressure Rheology for Quantitative Elastohydrodynamics*, 2nd Ed., Elsevier.

(10) Walters, C. T. (1971), "The Dynamics of Ball Bearings," *Journal of Lubrication Technology*, **93**, pp 1–10. doi:10.1115/1.3451516

(11) Gupta, P. K. (1979), "Dynamics of Rolling Element Bearings, Parts I, II, III and IV," *Journal of Lubrication Technology*, **101**, pp 293–326. doi:10.1115/1.3453357

(12) Gupta, P. K. (1984), *Advanced Dynamics of Rolling Elements*, Springer-Verlag. Related computer code, ADORE, Available at: www.PradeepKGuptaInc.com (accessed April 15, 2020).

(13) Gupta, P. K. (2011), "Current Status of and Future Innovations in Rolling Bearing Modeling," *Tribology Transactions*, **54**, pp 394–403. doi:10.1080/10402004.2010.551805

(14) Shevchenko, R. and Bolan, P. (1957), "A Visual Study of Ball Motion in High-Speed Thrust Bearing," **SAE Technical Paper 570244**. Accessed at: 10.4271/570244 (accessed April 15, 2020).

(15) Hirano, F. (1965), "Motion of a Ball in Angular-Contact Ball Bearing," *ASLE Transactions*, **8**, pp 425–434. doi:10.1080/05698196508972112

(16) Anderson, W. J. (1966), "Rolling Element Bearings," *Advanced Bearing Technology*, Bisson, E. E. and Anderson, W. J. (Eds.), ThirdPrinting, pp 159–164, National Aeronautics and Space Administration: Publication NASA SP-38.

(17) Kingsbury, E. P. (1968), "Ball Motion in Angular Contact Bearings," *Wear*, **11**, pp 41–50.

(18) Kingsbury, E. P. (1980), "Basic Speed Ratio of an Angular Contact Bearing," *Journal of Lubrication Technology*, **102**(3), pp 391–394. doi:10.1115/1.3251558

(19) Gupta, P. K. (1980), "Discussion of Basic Speed Ratio of an Angular Contact Bearing, by E.P. Kingsbury," *Journal of Lubrication Technology*, **102**(3), pp 391–394. doi:10.1115/1.3251559

(20) Ai, X. and Moyer, C. A. (2001), "Rolling Element Bearings," *Modern Tribology Handbook*, Bhushan, B. (Ed.), CRC Press.

(21) Gupta, P. K. (2002), "On a Kinematic Hypothesis for Angular Contact Ball Bearings," *ASTM Symposium on Rolling Element Bearings*, Orlando, FL, April 22–24.

(22) Gupta, P. K., Taketa, J. I., and Price, C. M. (2020), "Thermal Interactions in Rolling Bearings," Proceedings of the Institution of Mechanical Engineers - Part J: Journal of Engineering Tribology, ***234****(8), pp 1233–1253.*

(23) Gupta, P. K. (2020), "AdoreQS: Quasi-Static Equilibrium Solution." Accessed at: www.PradeepKGuptaInc.com/AdoreQS.html (accessed April 15, 2020).